

## Spatiotemporal Variability of Summer Precipitation in Southeastern Arizona

SUSAN STILLMAN AND XUBIN ZENG

*Department of Atmospheric Sciences, The University of Arizona, Tucson, Arizona*

WILLIAM J. SHUTTLEWORTH

*Department of Hydrology and Water Resources, The University of Arizona, Tucson, Arizona*

DAVID C. GOODRICH AND CARL L. UNKRICH

*Southwest Watershed Research Center, Agricultural Research Service, U.S. Department of Agriculture, Tucson, Arizona*

MAREK ZREDA

*Department of Hydrology and Water Resources, The University of Arizona, Tucson, Arizona*

(Manuscript received 18 January 2013, in final form 28 April 2013)

### ABSTRACT

The Walnut Gulch Experimental Watershed (WGEW) in southeastern Arizona covers  $\sim 150 \text{ km}^2$  and receives the majority of its annual precipitation from highly variable and intermittent summer storms during the North American monsoon. In this study, the patterns of precipitation in the U.S. Department of Agriculture–Agricultural Research Service (USDA-ARS) 88-rain-gauge network are analyzed for July through September from 1956 to 2011. Because small-scale convective systems generate most of this summer rainfall, the total ( $T$ ), intensity ( $I$ ), and frequency ( $F$ ) exhibit high spatial and temporal variability. Although subsidiary periods may have apparent trends, no significant trends in  $T$ ,  $I$ , and  $F$  were found for the study period as a whole. Observed trends in the spatial coverage of storms change sign in the late 1970s, and the multidecadal variation in  $I$  and spatial coverage of storms have statistically significant correlation with the Pacific decadal oscillation and the Atlantic multidecadal oscillation indices. Precipitation has a pronounced diurnal cycle with the highest  $T$  and  $F$  occurring between 1500 and 2200 LT, and its average fractional coverage over 2- and 12-h periods is less than 40% and 60% of the gauges, respectively. Although more gauges are needed to estimate area-averaged daily precipitation, 5–11 gauges can provide a reasonable estimate of the area-averaged monthly total precipitation during the period from July through September.

### 1. Introduction

The majority of the total annual rainfall in the Walnut Gulch Experimental Watershed (WGEW) in southeastern Arizona occurs in summer from highly localized convective storms associated with the North American monsoon (NAM). Consequently, most runoff, flooding, erosion, ephemeral channel recharge, and soil water replenishment occur during the summer months, with these processes depending not only on total rainfall but

also on the intensity and frequency of the precipitation events.

Globally, there are very few areas with sufficient observations to allow high-quality investigation of the spatial distribution of precipitation (Garcia et al. 2008). Houser et al. (1999) found, for example, that observed precipitation at gauges 6 km apart in the WGEW can be considered independent, indicating that accurate spatial distributions of precipitation and soil moisture are hard to quantify with a limited number of samples. It is well known that highly inhomogeneous terrain can easily produce large biases with just one sample gauge, and Xie and Arkin (1995) showed that increasing the number of gauges increases the estimation accuracy of  $2.5^\circ \times 2.5^\circ$  grid-box-averaged, 30-day precipitation. Kursinski and

---

*Corresponding author address:* Susan Stillman, The University of Arizona, Physics-Atmospheric Sciences Bldg., Rm. 542, 1118 E. 4th St., P.O. Box 210081, Tucson, AZ 85721-0081.  
E-mail: sstill88@email.arizona.edu

Zeng (2006) showed that for a  $200 \text{ km} \times 200 \text{ km}$  area in Ohio, different numbers of samples are required to make estimates of area-averaged total, intensity, and frequency, and results are dependent on the threshold precipitation rate.

Notwithstanding these observational challenges, in an analysis based on just six gauges in the WGEW, Nichols et al. (2002) concluded that between the years 1956 and 1996 there was an overall increase in summer precipitation frequency but a decrease in storm intensity, resulting in no observed trend in total precipitation. Goodrich et al. (2008) found the same result of no trend in total summer precipitation for the same six gauges as well as area-averaged total summer precipitation, which holds with 10 more years of precipitation data. Little research has been done on the relationship between climate indices and decadal and multidecadal characteristics of NAM precipitation, although Arias et al. (2012) speculated that the retreat dates of the NAM are related to the Atlantic multidecadal oscillation (AMO). Mantua and Hare (2002), who focused only on winter Pacific decadal oscillation (PDO) indices, found that warm PDO indices correspond with anomalously wet periods in the southwestern United States, defined by a significant correlation between PDO and precipitation. However, using instrument records and geostatistical modeling, Guan et al. (2005) suggested that summer total precipitation over northern New Mexico is not correlated to PDO.

Whereas Goodrich et al. (2008) examined spatial variability in terms of years to uniformity of total precipitation and computed trends in summer, nonsummer, and annual total precipitation, the current study will look at the interannual variability of the spatial distribution and trends in precipitation total, intensity, and frequency and will determine the spatial coverage of individual precipitation events. Kursinski and Zeng (2006) conducted similar analyses; however, they focused on a  $200 \text{ km} \times 200 \text{ km}$  area over the U.S. Midwest using data from two summers, and this study will focus on a much smaller watershed over the NAM region from 56 summers.

The goal of this study is to quantify the spatiotemporal variations of precipitation using rainfall data from the dense network of rain gauges in the WGEW. Three questions will be addressed: (1) What, if any, are the trends in precipitation amount, frequency, and intensity? (2) Are there multidecadal time variations in precipitation characteristics in this region that are possibly related to climate indices? and (3) How many rain gauges are needed to estimate area-averaged precipitation? Section 2 describes the dataset and analysis methods, section 3 presents the results, and section 4 contains conclusions.

## 2. Dataset and analysis methods

The WGEW is a tributary watershed of the San Pedro River watershed, which covers an area of approximately  $150 \text{ km}^2$  surrounding Tombstone in southeastern Arizona. The watershed is spatially heterogeneous, with elevation ranging from 1250 to 1585 m, and the dominant vegetation covers of shrub and grassland are typical of rangeland in the semiarid U.S. Southwest. The northeast corner of the watershed lies in the flanks of the Dragoon Mountains and the western border is in the Tombstone hills. The soils are predominantly sandy, gravely loams with slopes ranging from 0% to 70%. The catchment is in a semiarid region with an average annual precipitation of 350 mm, approximately 60% of which occurs during the months July–September (Keefer et al. 2003).

The U.S. Department of Agriculture–Agricultural Research Service (USDA-ARS) Southwest Watershed Research Center maintains a suite of instruments in WGEW that currently includes 88 rain gauges located mainly within the watershed with others closely surrounding it, making it one of the most densely instrumented watersheds with an area greater than  $10 \text{ km}^2$  (Goodrich et al. 2008; Garcia et al. 2008). The gauges, which provide precipitation data at 1-min intervals, have been in use since 1956. Initially, analog gauges collected data in the form of digitized charts, but they were replaced by digital gauges with lower measurement and timing errors in 2000. Although the measurement errors are larger in the analog gauges, Keefer et al. (2008) concluded that the 30-min precipitation characteristics, which are used in this study, are essentially equivalent in the analog and digital gauges. Figure 1 illustrates the progressive installation of the 88 gauges currently gathering precipitation data in the WGEW. Throughout the 56 yr, gauges were installed and removed, and the numbers of gauges that were available for the years indicated in Fig. 1 are 44 in 1956, 84 in 1966, 84 in 1976, and 73 in 1986. In the early 1980s, there were 88 gauges, most of which were available in most years through 2011, 1986 being one of the exceptions during which several gauges were turned off. The average distance between nearest neighboring gauges is well within the 6-km distance suggested by Houser et al. (1999) as the criterion for independent precipitation observations.

In this study, the 1-min rainfall data were averaged to 30 min [this is to be consistent with the soil moisture measurements used in a separate study (S. Stillman et al. 2013, unpublished manuscript)]. This was done by turning the original breakpoint data into time series with 1-min time steps and binning the data into 30-min intervals. The present analysis focuses on precipitation in

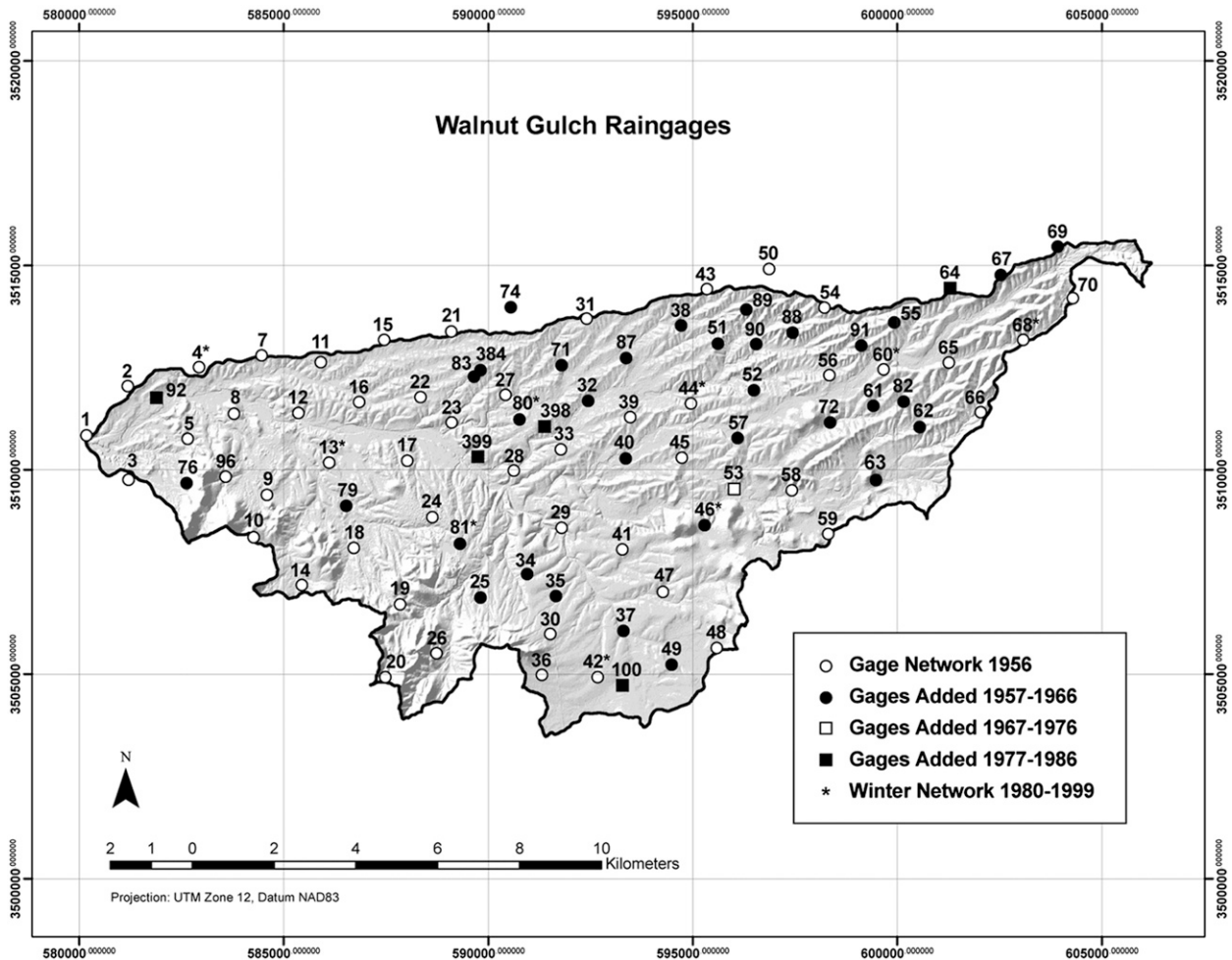


FIG. 1. Location of all rain gauges that were installed in 1956 and in subsequent 10-yr increments over the WGEW. The WGEW is located approximately 150 km southeast of Tucson, Arizona. The winter network refers to the nine gauges that continued to collect data while the rest were shut down from 1 January through 1 June in the years 1980–99.

July–September for which we compute the total rainfall amount ( $T$ ), the intensity ( $I$  minus  $T$  divided by the number of 30-min measurements with precipitation), and frequency ( $F$ ) or the fraction of time with precipitation occurrence (the number of 30-min intervals with precipitation divided by the total number of 30-min intervals). Clearly, the value of  $T$  for July–September of each year is equal to the product of  $I$  and  $F$  times the number of 30-min intervals over the time period. While  $T$  is independent of the measurement interval used,  $I$  and  $F$  depend on the selected measurement interval. This may be significant for the short-lived, intense convective storms that characterize the NAM because selecting shorter measurement intervals could result in higher intensities and lower frequencies. The computed values of  $T$ ,  $I$ , and  $F$  may also be sensitive to  $p_{\text{crit}}$ , the minimum precipitation amount that the gauges can report (by decreasing  $T$  and  $F$  and increasing  $I$  with the

increase of  $p_{\text{crit}}$ ): in this analysis,  $p_{\text{crit}} > 0.254$  mm (0.01 in) in each 30-min interval. For some aspects of the analysis, the precipitation ( $T$ ,  $I$ , and  $F$ ) data for all of the gauge sites were spatially interpolated onto  $100\text{ m} \times 100\text{ m}$  grid cells covering the WGEW using an inverse distance weighted interpolation scheme following Garcia et al. (2008). In this study, we used a second-order, two-dimensional interpolation in which the weighting given to each gauge is inversely proportional to the square of its distance from the grid box.

### 3. Results and discussion

Figure 2 illustrates the significant temporal variability of the July–September precipitation  $T$ ,  $I$ , and  $F$  averaged over all of the grid cells in the WGEW, and these values agree well with the all-gauge-averaged values. The quantity  $T$  derived as a grid average, for example, varies

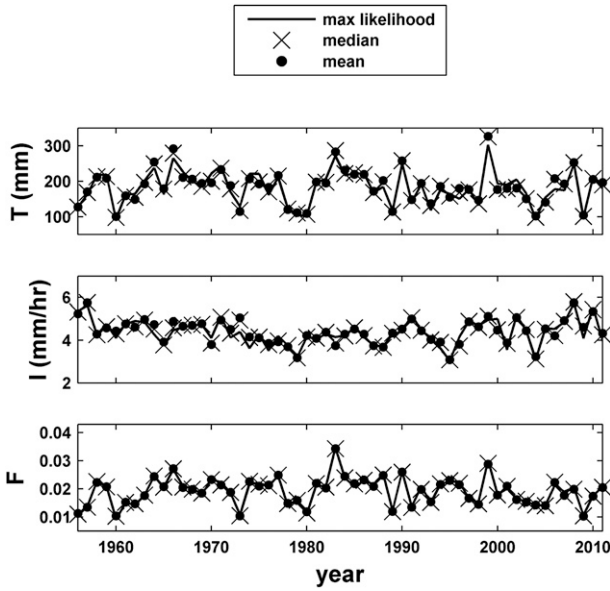


FIG. 2. The 1 July to 30 September spatial mean, median, and maximum likelihood values (found temporally at each grid cell and then averaged spatially) of precipitation (top to bottom) total, intensity, and frequency. These values nearly overlap in each year.

from 95.9–325.8 mm; this is very similar to the all-gauge-averaged total precipitation, which varies from 93.6 to 321.9 mm. Figure 2 shows that the mean, most frequent (defined as the peak of a 30-bin histogram), and median values of precipitation also agree well with each other.

Linear regression of the median values of  $T$ ,  $I$ , and  $F$  from 1956 to 2011 reveals no significant trends, agreeing with Goodrich et al. (2008) on the trend of  $T$  for the period from 1956 to 2006. As previously mentioned, Nichols et al. (2002) found a statistically significant positive trend in  $F$  and negative trend in  $I$  between 1956 and 1996 based on an analysis of six rain gauges. During the period between 1956 and 1996 our results (Fig. 2) are consistent with the Nichols et al. (2002) results. The trend in the median of  $F$  and  $I$  are, respectively,  $1.07 \times 10^{-3}$  ( $p = 0.11$ ) and  $-0.23 \text{ mm h}^{-1}$  (statistically significant with  $p = 9 \times 10^{-4}$ ) per decade over this period. However, the trends between 1956 and 1996 are not representative of the period between 1956 and 2011, during which trends are an order of magnitude smaller and are not statistically significant. This illustrates the critical importance of using a long period of data in the computation of trends in precipitation intensity and frequency. This is in agreement with the results found by Anderson et al. (2010) over the core monsoon region (Arizona and western New Mexico).

The spatial distributions of  $T$ ,  $I$ , and  $F$  across the WGEW were calculated for each year. Figure 3 shows an example for a dry year (1960) where  $T$ ,  $I$ , and  $F$  vary in the ranges of 52.3–151.7 mm, 3–6.25  $\text{mm h}^{-1}$ , and 0.007–0.014, respectively. In contrast for a wet year (1999), the intensity ( $I$ ) has less spatial variation in the range 4.45–6.06  $\text{mm h}^{-1}$ , while  $F$  is generally higher, varying from 0.023–0.032 (Fig. 3). Over the period from

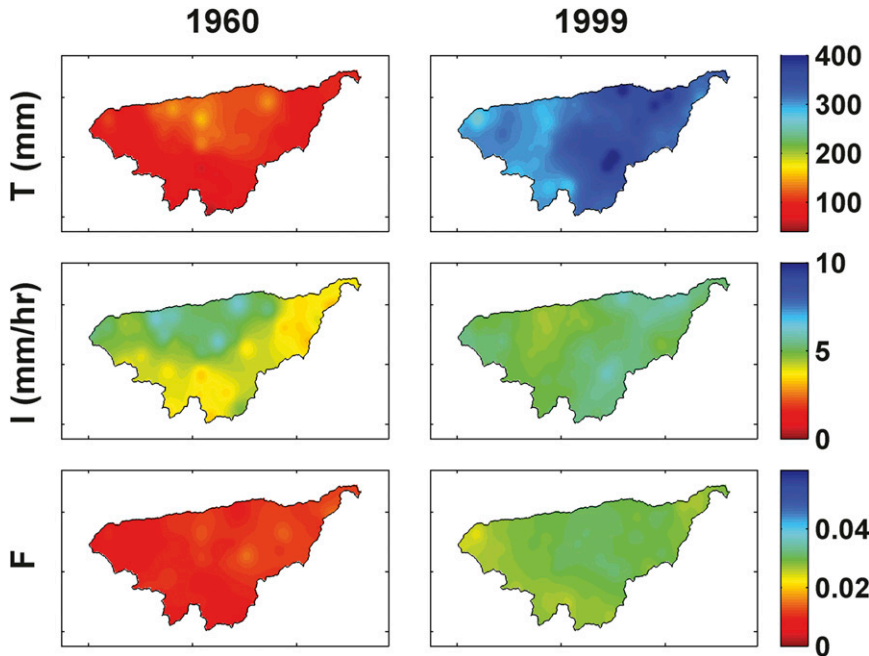


FIG. 3. July–September total (top to bottom) precipitation (mm), intensity ( $\text{mm h}^{-1}$ ), and frequency for (left) a dry year (1960) and (right) a wet year (1999).

1956 to 2011, on average, as found in Goodrich et al. (2008), there is a slight increase in  $T$  from west to east. Partly because of the mountains bordering the watershed on the northeast and west sides, there is also a west to east increase in intensity, and frequency is highest on the western boundary and lowest in the north-central region.

Interannual relationships between  $T$ ,  $I$ , and  $F$  are computed by first calculating these values each year for each gauge. The correlation of area-averaged (all gauges) frequency to area-averaged total is higher than that of intensity, with correlation values of 0.86 and 0.26, respectively, suggesting that while  $T$  is affected by the average intensity of the individual storms, it is more dependent on the frequency of precipitation. To evaluate the interannual variability of the spatial heterogeneities shown in Fig. 3, for each year we computed the coefficients of (spatial) variation (i.e., the normalized spatial standard deviations) of  $T$ ,  $I$ , and  $F$ . The years with highest precipitation totals were found to have the least spatial heterogeneity in precipitation  $T$ ,  $I$ , and  $F$  (with the interannual correlation of  $T$  with the normalized spatial standard deviation of  $T$ ,  $I$ , and  $F$  of  $-0.47$ ,  $-0.35$ , and  $-0.55$ , respectively), which suggests that the highest total precipitation across the WGEW tends to occur during years with large storm systems that may cover the entire watershed.

The average value of rainfall intensity across the WGEW in the July–September period can be calculated as the spatial average of the interpolated value of  $I$  for all grid cells (Fig. 3). It can also be computed as the average value of  $I$  from each gauge. The latter is done in two ways: as the spatial average of the individual gauge intensities (denoted as local average,  $I_{loc}$ ), or as the intensity of the spatially (all gauge) averaged 30-min precipitation rate (denoted as area average,  $I_{area}$ ). Figure 4 shows that  $I_{loc}$  varies from 3.07 to 5.78 mm h<sup>-1</sup> and that  $I_{area}$  varies from 0.59 to 1.61 mm h<sup>-1</sup>, and the ratio of  $I_{loc}/I_{area}$  varies from 3.16 to 7.31. This result is broadly consistent with the order of magnitude of the difference between the two averages found by Kursinski and Zeng (2006) over a much larger (200 km × 200 km) homogeneous area in Ohio, United States.

The area-averaged intensity is lower because it involves averaging the 30-min precipitation of all gauges, some of which may receive no measured rainfall during a 30-min period. The greater the difference between  $I_{loc}$  and  $I_{area}$ , the more spatially heterogeneous the precipitation pattern, and the results given in Fig. 4 clearly indicate that during the NAM, convective precipitation is indeed spatially heterogeneous across the 150 km<sup>2</sup> area of the WGEW. To better quantify this heterogeneity, we calculated the spatial coverage of storms in the

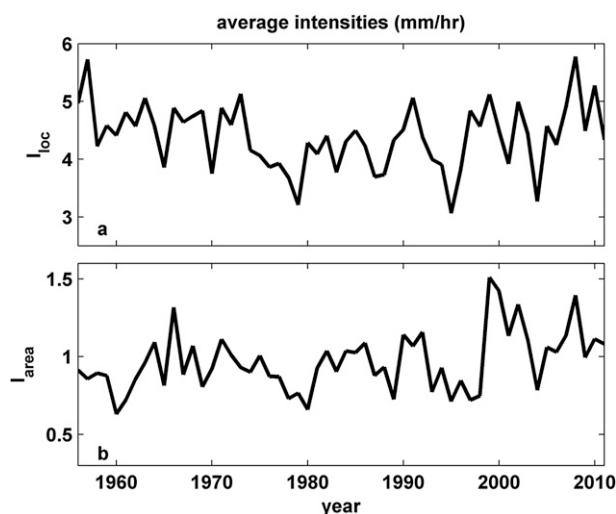


FIG. 4. Interannual variability of spatial average of July–September precipitation (a) intensities at all gauge sites ( $I_{loc}$ ) and (b) intensity of 30-min precipitation ( $I_{area}$ ).

monsoon season for selected period in Fig. 5. In each year, the fractional coverage is calculated as the time average of the fraction of gauges that received any precipitation over a prescribed time interval (2 and 12 h in Fig. 5) during which there was recorded precipitation somewhere in WGEW. For a 2-h interval, the average coverage is never greater than 40%, and even for a 12-h interval, the average fractional coverage during the monsoon season peaks at around 60%. Since the lifespan of convective precipitation is usually within two hours, the convective precipitation fractional coverage as used in the canopy interception computation in regional models with a grid spacing of  $\sim 12$  km should be less than 0.4 over the southwestern United States. It is interesting to note that the fractional spatial coverage of storms peaks in the late 1970s (Fig. 5), while the value of  $I$  is relatively small during this period (Fig. 2). The mechanisms for this and for the abrupt jump in the fractional spatial coverage in some years (e.g., in late 1990s for the 2-h interval) are unclear at present and require further analysis.

The PDO and AMO indices are recognized as characterizing important modes of variability in the earth system at the multidecadal time scale. The PDO index is computed as the first principal component of North Pacific sea surface temperature (SST) variability (<http://jisao.washington.edu/pdo/>), while the AMO index is computed as the detrended weighted average SST anomalies over the North Atlantic (<http://www.esrl.noaa.gov/psd/data/timeseries/AMO/>). McCabe et al. (2004) showed that drought frequency in the United States is highly related to AMO and PDO. Correlation analysis of precipitation

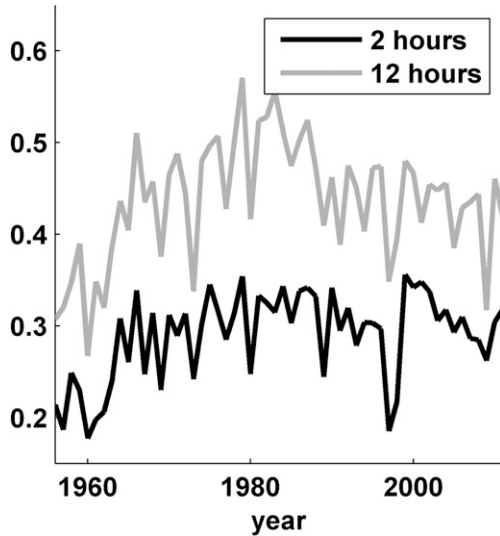


FIG. 5. Average fraction of gauges that received precipitation during storm events for time intervals of 2 and 12 h when any precipitation occurred within the watershed.

characteristics in the WGEW shows a correlation of  $I$  with the PDO of  $-0.46$ , which is significant at the 0.01 level. Similarly, correlations of the 12-h storm coverage with the AMO and PDO indices are  $-0.38$  and  $0.32$  (both significant at the 0.01 level). The correlation of  $F$  and the AMO is  $-0.24$  (significant at the 0.05 level only). In contrast, the correlations of  $T$  with both the PDO and AMO indices are not significant, and the correlations of  $I$  with the AMO index and  $F$  with the PDO index are also not significant.

When analyzing the diurnal cycle of precipitation, we first computed  $T$ ,  $I$ , and  $F$  for each half hour in the months from July through September at each gauge site: these are shown as gray lines in Fig. 6. These quantities can alternatively be computed using 30-min precipitation averaged over all gauges, shown as the black solid lines in Fig. 6. The maximum frequency of precipitation occurs at 1600 LT (Fig. 6b), with a broader maximum in precipitation amount between 1500 and 2200 LT (Fig. 6a). Between the hours of 0200 and 1200 LT, precipitation intensity is fairly constant and low (Fig. 6c). The average gauge intensity (frequency) is lower (higher) than the individual intensities (frequencies) because of the limited spatial coverage of individual convective storms within the catchment (also shown in Figs. 4, 5). This suggests that  $I$  and  $F$  derived from individual gauges cannot be used to reliably evaluate these values for area-averaged precipitation (as calculated by weather and climate models, for example). To explore the interannual variability of the diurnal cycle given in Fig. 6, Fig. 7 shows the hour of maximum precipitation frequency for each

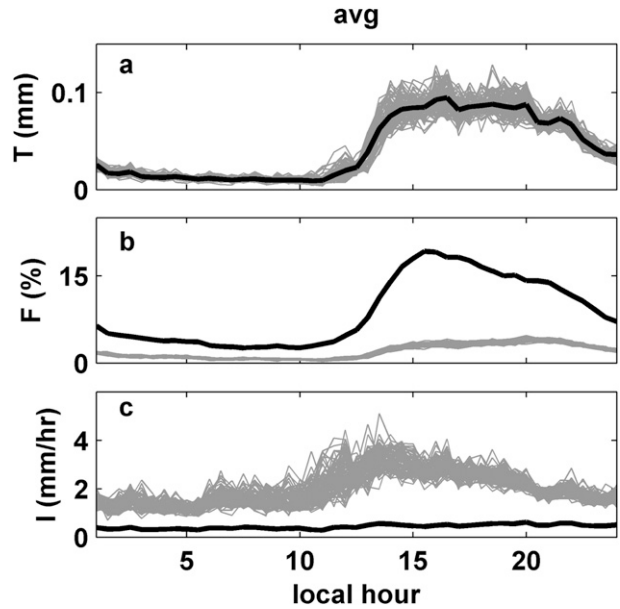


FIG. 6. Averaged diurnal cycle of 30-min precipitation (top to bottom) amount, frequency, and intensity over the whole period for each gauge (gray lines) and for the all-gauge average (black lines).

gauge and for the all-gauge average for each year between 1956 and 2011. The maximum frequency of all-gauge-averaged precipitation always occurs during mid- to late afternoon hours, while the timing of maximum frequency for individual gauges falls around this time or later in the day, and occasionally in the hours after midnight.

Following Kursinski and Zeng (2006) and Xie and Arkin (1995), Fig. 8 illustrates the number of gauges needed to make a reliable estimate of area-averaged precipitation over the aggregation periods of 1 and 30 days. For each number of gauges  $n$  (between 1 and 50),  $n$  gauges were randomly selected 50 times from the 88 gauges, and the standard deviation of the difference

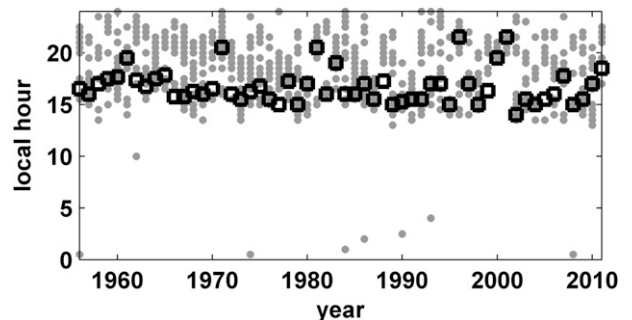


FIG. 7. Local hour with maximum frequency of precipitation for each gauge (gray dots) and for the all-gauge average (black outlined squares).

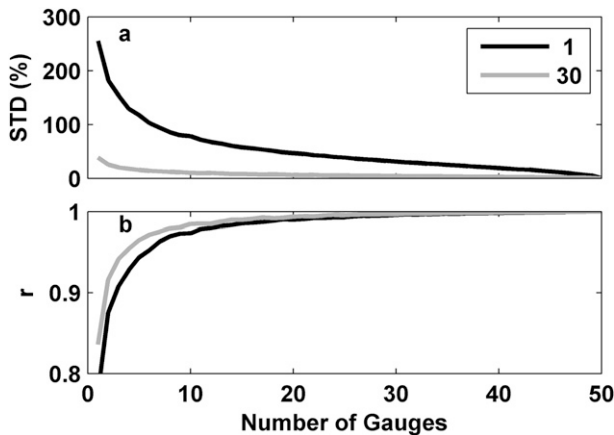


FIG. 8. (a) Relative uncertainty (defined in the text) and (b) correlation of estimates to actual precipitation for 1- and 30-day total precipitation vs gauge numbers.

between the  $n$ -gauge-averaged and all-gauge-averaged precipitation was then computed. This value normalized by the all-gauge-averaged precipitation represents the relative uncertainty. For example, 18 gauges are required for the estimated area-averaged daily averaged precipitation with 50% relative uncertainty (Fig. 8a), but when estimating 30-day-averaged precipitation, only 11 gauges are required for 10% uncertainty in area-averaged precipitation. The correlation between estimates of area-averaged precipitation made with a limited number of gauges and the all-gauge-averaged precipitation (Fig. 8b) increases more rapidly with gauge number than the decrease in the standard deviation (Fig. 8a). Furthermore, the correlation is similar for the daily and 30-day precipitation, while the standard deviation is quite different for daily and 30-day-averaged precipitation. To reach a correlation of 0.95, five gauges are needed for both the daily and 30-day-averaged precipitation estimates, this being similar to the number of gauges (five) reported in Xie and Arkin (1995) and Kursinski and Zeng (2006) for estimates over much larger  $2.5^\circ \times 2.5^\circ$  and  $200 \text{ km} \times 200 \text{ km}$  areas.

As mentioned earlier, gauges were intermittently removed and installed so that there was a minimum of 37 available gauges from July to September in any year. As results (e.g., those in Figs. 2–7) may be affected by the density of measurement, we repeated the above analyses using 56 gauges that were available for at least 50 yr (90%) of the study period and found that the above conclusions are not affected. For instance, while the range of values of the all-gauge- and grid-averaged precipitation is slightly smaller (97.1–314.9 mm and 101–321 mm, respectively), the trends found are almost the same. In the period 1956–2006, the trends in  $I$  and  $F$  are  $-0.25 \text{ mm h}^{-1} \text{ decade}^{-1}$  and  $1.06 \times 10^{-3} \text{ decade}^{-1}$  and

are significant, and for the period 1956–2011, as with the all-gauge trend analysis, these trends disappear. The fractional coverage still peaks in the late 1970s where  $I_{\text{loc}}$  and  $I_{\text{area}}$  are relatively low. The significant correlations found between climate indices and precipitation characteristics remain significant, and no new significant correlations are found when the consistent 56 gauges are used as opposed to the full set.

#### 4. Conclusions

The Walnut Gulch Experimental Watershed (WGEW) in Southeastern Arizona with a drainage area of  $\sim 150 \text{ km}^2$  is subject to highly variable and intermittent summer precipitation during the North American monsoon. The spatial and temporal variability of 30-min-averaged precipitation measured with 88 rain gauges distributed across the WGEW were analyzed during the period from July through September between 1956 and 2011. The primary results of this analysis are as follows.

- 1) The spatially averaged total precipitation, precipitation intensity, and frequency of precipitation from July through September show large interannual variability. The trend toward increasing frequency and decreasing intensity in precipitation for the period of 1956–96 reported in previous research which used just 6 gauges was also observed in this analysis of 88 gauges. However, these trends do *not* persist when the time period of analysis is extended through to 2011. This result emphasizes the importance of using adequately long-term datasets in trend assessment.
- 2) The spatial average precipitation correlates with the normalized spatial standard deviation of total, intensity, and frequency. The grid-averaged total precipitation is more highly correlated with grid-averaged frequency than with grid-averaged intensity. Most precipitation events do not cover the entire watershed, and the average fractional coverage of rainfall over 2- and 12-h periods is less than 40% and 60% of the gauges, respectively.
- 3) A possible multidecadal pattern in intensity and average storm coverage was found with a sign change of trend in late 1970s. Correlations of precipitation intensity with PDO and storm coverage with PDO and AMO are statistically significant (at the 0.01 and 0.05 levels), but correlations of precipitation amount with AMO and PDO are insignificant.
- 4) Gauge precipitation amount and frequency are highest between 1500 and 2200 LT, and spatially averaged precipitation is most frequent over the WGEW at 1600 LT. Storms between the hours of 0200 and 1200 LT have very low intensity.

- 5) To reasonably estimate area-averaged precipitation amount, 5–11 gauges are needed for monthly precipitation, but more gauges are needed for daily precipitation.

*Acknowledgments.* All the instruments used in this research are owned and operated by USDA-ARS: the precipitation data used were obtained from the organization's website (<http://www.tucson.ars.ag.gov/dap/>), and we express our sincere thanks to the staff of the USDA-ARS Southwest Watershed Research Center for their effort and dedication in producing the long-term, high-quality data set used in this analysis. This research was supported by NSF (AGS-0838491 for the COSMOS project; EF-1238908 for the macrosystems project).

#### REFERENCES

- Anderson, B. T., J. Wang, G. Salvucci, S. Gopal, and S. Islam, 2010: Observed trends in summertime precipitation over the southwestern United States. *J. Climate*, **23**, 1937–1944, doi:10.1175/2009JCLI3317.1.
- Arias, P. A., R. Fu, and K. C. Mo, 2012: Decadal variation of rainfall seasonality in the North American monsoon region and its potential cause. *J. Climate*, **25**, 4258–4274, doi:10.1175/JCLI-D-11-00140.1.
- Garcia, M., C. D. Peters-Lidard, and D. C. Goodrich, 2008: Spatial interpolation of precipitation in a dense gauge network for monsoon storm events in the southwestern United States. *Water Resour. Res.*, **44**, W05S13, doi:10.1029/2006WR005788.
- Goodrich, D. C., T. O. Keefer, C. L. Unkrich, M. H. Nichols, H. B. Osborn, J. J. Stone, and J. R. Smith, 2008: Long-term precipitation database, Walnut Gulch Experimental Watershed, Arizona, United States. *Water Resour. Res.*, **44**, W05S04, doi:10.1029/2006WR005782.
- Guan, H., E. R. Vivoni, and J. L. Wilson, 2005: Effects of atmospheric teleconnections on seasonal precipitation in mountainous regions of the southwestern U.S.: A case study in northern New Mexico. *Geophys. Res. Lett.*, **32**, L23701, doi:10.1029/2005GL023759.
- Houser, P. R., D. C. Goodrich, and K. H. Syed, 1999: Case Study: Runoff, Precipitation, and Soil Moisture at Walnut Gulch. *Spatial Patterns in Catchment Hydrology: Observations and Modeling*, R. Grayson and G. Bloschl, Eds., Cambridge University Press, 125–157.
- Keefer, T. O., and Coauthors, 2003: Southwest Watershed Research Center and Walnut Gulch Experimental Watershed. SWRC Publ. Reference No. 1588, 40 pp. [Available online at <http://www.tucson.ars.ag.gov/unit/publications/PDFfiles/1588.pdf>.]
- , C. L. Unkrich, J. R. Smith, D. C. Goodrich, M. S. Moran, and J. R. Simanton, 2008: An event-based comparison of two types of automated-recording, weighing bucket rain gauges. *Water Resour. Res.*, **44**, W05S12, doi:10.1029/2006WR005841.
- Kursinski, A. L., and X. Zeng, 2006: Areal estimation of intensity and frequency of summertime precipitation over a midlatitude region. *Geophys. Res. Lett.*, **33**, L22401, doi:10.1029/2006GL027393.
- Mantua, N. J., and S. R. Hare, 2002: The Pacific decadal oscillation. *J. Oceanogr.*, **58**, 35–44, doi:10.1023/A:1015820616384.
- McCabe, G. J., M. A. Palecki, and J. L. Betancourt, 2004: Pacific and Atlantic Ocean influences on multidecadal drought frequency in the United States. *Proc. Natl. Acad. Sci. USA*, **101**, 4136–4141, doi:10.1073/pnas.0306738101.
- Nichols, M. H., K. G. Renard, and H. B. Osborn, 2002: Precipitation changes from 1956 to 1996 on the Walnut Gulch Experimental Watershed. *J. Amer. Water Resour. Assoc.*, **38**, 161–172, doi:10.1111/j.1752-1688.2002.tb01543.x.
- Xie, P., and P. A. Arkin, 1995: An intercomparison of gauge observations and satellite estimates of monthly precipitation. *J. Appl. Meteor.*, **34**, 1143–1160, doi:10.1175/1520-0450(1995)034<1143:AIOGOA>2.0.CO;2.